ELECTROCHEMICAL REDUCTION OF DODECYLPYRIDINIUM BROMIDE IN APROTIC SOLVENTS: MECHANISTIC STUDIES

Magdaléna HROMADOVÁ[1,*], Lubomír POSPÍŠIL[2], Romana SOKOLOVÁ[3] and Viliam KOLIVOŠKA[4]

J. Heyrovský Institute of Physical Chemistry, Academy of Sciences of the Czech Republic, v.v.i., Dolejškova 3, 182 23 Prague 8, Czech Republic; e-mail: [1] hromadom@jh-inst.cas.cz, [2] pospisil@jh-inst.cas.cz, [3] romana.sokolova@jh-inst.cas.cz, [4] viliam.kolivoska@jh-inst.cas.cz

Received August 2, 2011
Accepted September 9, 2011
Published online January 26, 2012

Paper submitted for a special issue of CCCC devoted to "distinguished followers of the J. Heyrovský School of Polarography". This work is dedicated to Professor Petr Zuman in celebration of his 85th birthday and to Professor Robert Kalvoda, who passed away on 2nd August, 2011, and to Professor Jiří Volke, who passed away on 17th October, 2011. Prof. Zuman is worldwide recognized authority in the field of organic electrochemistry. Prof. Kalvoda contributed immensely to the development of modern electrochemical instrumentation techniques applied in this communication. Prof. Volke made significant contribution to understanding of the redox mechanisms of pyridine and pyridinium compounds.

Reduction mechanism of 1-dodecylpyridin-1-ium bromide (DPBr) in dimethylsulfoxide has been studied on mercury electrode. Based on the classical polarographic methods as well as on the use of AC techniques it was shown that DPBr is reduced in a reversible one electron transfer step followed by dimerization of the corresponding radical species. Reduction process is accompanied by the adsorption phenomena even in the non-aqueous solvents. Possible modes of DPBr adsorption have been studied by the ex situ scanning tunnelling microscopy (STM) imaging of these molecules on highly oriented pyrolytic graphite.
Keywords: Dodecylpyridinium reduction; Dodecylpyridinium bromide; Reduction; Spectroelectrochemistry; Scanning tunnelling microscopy; Mechanistic studies; Electron transfer.

This work is devoted to detailed studies of the reduction mechanism of 1-dodecylpyridin-1-ium bromide (DPBr) in aprotic solvents. Such data are relevant in view of the fact that alkylpyridinium salts are the electrochemical precursors of dialkyl viologens, which represent one of the simplest models of conducting organic molecular wires studied up to date[1–7]. More complex structures of so-called extended viologens are currently under in-

doi:10.1135/cccc2011154

vestigation as potential examples of the real "molecular wires" in the emerging field of molecular electronics[8,9].

Redox properties of *N*-alkylpyridinium salts have been studied primarily in the aqueous solutions[10–18]. In neutral and alkaline aqueous solutions, *N*-alkylpyridinium salts are reduced by one-electron to the corresponding radicals. Electron transfer in alkaline solutions is followed by a dimerization process with reported bimolecular dimerization constant in excess of 1×10^7 l mol^{-1} s^{-1} (Scheme 1)[11,16]. Anodic oxidation of the reduction products, tetrahydrobipyridine dimers, gives a mixture of alkylpyridinium salts and 1,1′-dialkyl-4,4′-bipyridinium cation (alkyl viologen)[19].

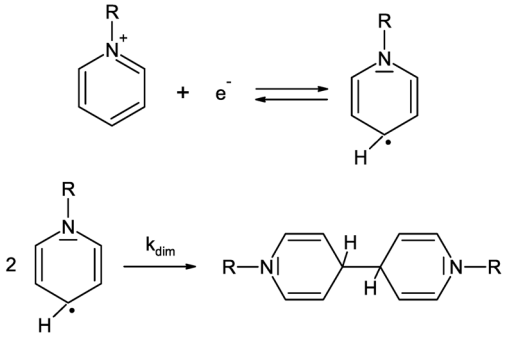

SCHEME 1

The reductive dimerization of 1-methylpyridinium salts, followed by oxidation of the product, has been used for the synthesis of herbicide paraquat (dimethyl viologen)[20]. It is interesting to point out that some authors obtained only the original pyridinium cation after the anodic reoxidation of the reduction product[17,18,21]. This was explained by the existence of two dimer isomers: one of them being tetrahydrobipyridine compound and the other the charge transfer complex formed by two radical intermediates[19].

Mairanovskii observed a positive shift of the half-wave potential with increasing concentration of *N*-methylpyridinium salts (20 mV for a ten-fold increase) and with increasing drop time. This finding was consistent with dimerization of the reduction product and the formation of reductively inactive species. The dimerization constant of 1×10^6 l mol^{-1} s^{-1} was reported[13]. Volke and Naarová[16] studied the reduction of the first five homologues of *N*-alkylpyridinium salts in alkaline aqueous solutions. All five cations gave a single reduction wave, which shifted to less negative potential with increasing length of the alkyl chain. The half-wave potential of all studied species was a function of concentration and drop time. The authors suggested that the reduction proceeds through one electron transfer with

subsequent dimerization of the radical to 1,1′-dialkyl-4,4′-tetrahydrobipyridine product[16]. They stated that the product reacts further both chemically and electrochemically, key intermediate in all subsequent reactions being the corresponding viologen radical. For example, 1,1′-dimethyl-4,4′-tetrahydrobipyridine product reacts with water molecules to give dimethyl viologen[18]. If the alkylpyridinium backbone contains bulky substituents at the positions 2, 4 and 6 the reduction proceeds via two reversible one-electron reduction steps and the dimer formation is prevented[22]. Instead, the comproportionation between the product and starting material is feasible.

Strong adsorption of the reactants as well as of the products is known to be operative in the aqueous solutions, whereas adsorption processes are greatly influenced by the polarity of solvent[14,16,23,24]. Kůta et al.[14] reported on the adsorption properties of DPBr. The maximum surface excess of the reactant on the electrode surface was estimated to be 1.3×10^{-10} mol cm^{-2} assuming the diffusion coefficient $D_{\mathrm{DPBr}} = 6 \times 10^{-6}$ cm^2 s^{-1}.

Only few works reported on the reduction of pyridinium cations in organic solvents[25–28]. Santhanam and Elving[25] studied the reduction properties of 1-substituted 3-nicotinamides in acetonitrile and DMSO. After the formation of pyridinyl radical through an uptake of one electron a rapid dimerization to tetrahydrobipyridine species was observed. The dimers showed greater stability in nonaqueous media compared to the aqueous one. Oxidation of the dimer gave back the original species[25]. The same effect was observed for the reduction of 1-methylpyridinium ion in acetonitrile[26]. Volke et al.[28] studied the substituted pyridinium cations by the phenyl groups in the positions 2, 4 and 6 in dimethylformamide, acetonitrile and dimethylsulfoxide solvents. An overall two electron reduction of substituted pyridinium cation was observed instead of the dimerization process.

It is surprising that the redox properties of the alkylpyridinium cations bearing long alkyl chains were not studied in organic solvents since such an approach eliminates the formation of micellar solutions and greatly simplifies the system studied. Aprotic solvents are frequently used to minimize the adsorption of reactants at the electrode| electrolyte interface and in our case DMSO was used in order to avoid the micelle formation in the solution bulk. DPBr is a cationic surfactant[29,30] that forms micellar solutions in aqueous and mixed media, whereas there is no literature record of the micelle formation in DMSO. Therefore, no micelles should be formed in our system in the concentration range studied.

This work presents mechanistic studies of the electrochemical reduction of DPBr in non-aqueous solvents on mercury, platinum mesh and highly oriented pyrolytic graphite (HOPG) electrodes as a model system using a combination of DC and AC electrochemical and spectroelectrochemical methods with ex situ scanning tunnelling microscopy (STM) analysis of DPBr adsorption. Even though the electrochemistry of the short chain alkylpyridinium cations has been studied in the past we are not aware of such work in the case of the long alkyl chain substituted pyridinium cations in DMSO. Finally, the paper deals with possible arrangements of the DPBr molecules on the HOPG electrode surface, which were visualized by the ex situ STM technique.

EXPERIMENTAL

Dodecylpyridinium bromide (DPBr) was kindly supplied by Institute of Physical Chemistry, Jena (Germany) and was dried before use. It is the same compound as that used by Kůta et al.[14]. Tetrabutylammonium hexafluorophosphate ($TBAPF_6$) was obtained from Sigma and was dried before use. Dimethyl sulfoxide, anhydrous, 99.9% (Sigma) was used as received. The water content was less than 50 ppm based on the Karl Fischer titration. Acetonitrile, anhydrous, 99.8% (Sigma) was used as received.

Electrochemical measurements were done using an electrochemical system for cyclic voltammetry, phase-sensitive AC polarography, and DC polarography. It consisted of a fast rise-time potentiostat and a lock-in amplifier (model SR830, Stanford Research Systems, USA). The instruments were interfaced to a personal computer via an IEEE-interface card (PC-Lab, AdvanTech Model PCL-848) and a data acquisition card (PCL-818) using 12-bit precision. A three-electrode electrochemical cell was used. The reference electrode (Ag|AgCl| 1 M LiCl) was separated from the test solution by a salt bridge with double-fritted junction. The working electrode was a valve-operated static mercury drop electrode (SMDE2, Laboratorní Přístroje, Prague) with an area either 2.73×10^{-3} or 1.036×10^{-2} cm^2. The auxiliary electrode was cylindrical platinum net. Oxygen was removed from the solution by passing a stream of argon. Cyclic voltammetry data were simulated using DigiSim 3.03b software (Bioanalytical Systems, Inc., USA).

The prototype of the spectroelectrochemical OTTLE (optically-transparent thin-layer electrode) cell was developed in the J. Heyrovský Institute and its construction was fully described by Krejčík et al.[31]. In these experiments, a modified version of the cell was purchased from the Department of Chemistry, University of Reading, UK [32], where the dismountable cell Specac, model Omni-Cell GS01800 (Specac Ltd., Orpington, UK) was adapted. The inlet and the outlet openings allow filling the cell with degassed samples under anaerobic conditions. Cyclic voltammograms were recorded using potentiostat/galvanostat Autolab 101 (Metrohm Autolab, the Netherlands), whereas the spectra were sampled every 2 s using a diode-array UV-Vis spectrometer Agilent, model 8453. Scanning tunneling microscopy images were obtained with the Nanoscope II STM station (Digital Instruments, USA). Highly oriented pyrolytic graphite (Grade SPI-1, SPI Supplies/Structure Probe, Inc., U.S.A.) was used for ex situ STM measurements.

RESULTS AND DISCUSSION

Several electrochemical methods (DC and AC polarography, voltammetry, UV-Vis spectroelectrochemistry, electrochemical impedance techniques) have been chosen for detailed investigation of the DPBr reduction in dimethylsulfoxide (DMSO). Figure 1a shows selected DC polarograms of DPBr in 0.1 M $TBAPF_6$ and DMSO at different DPBr concentrations. Only one reduction wave was observed for all DPBr concentrations studied, i.e., in the range from 10^{-6} to 10^{-3} mol l^{-1}, no adsorption prewaves or postwaves have been detected at these experimental conditions. The limiting DC polarographic current increases linearly with increasing DPBr concentration yielding the slope (9.99 ± 0.06) × 10^{-4} A l mol^{-1}. The half-wave potential shifts towards more positive values with increasing DPBr concentration (Fig. 1b) and the slope of the dependence gives the value 21 ± 1 mV. These findings point to the second order reaction following the electron transfer step.

As with shorter *N*-alkylpyridinium cations one may expect the formation of dimers after a reversible uptake of the first electron. The shape of the polarographic wave in the case of a bimolecular reaction following the reversible one-electron reduction is according to Hanuš[33,34] given by the following expression

$$E = E^0 - \frac{2.303RT}{F} \log \frac{i^{2/3} i_d^{1/3}}{i_d - i} + \frac{2.303RT}{3F} \log \frac{ck_2 t}{1.51} \qquad (1)$$

with the half-wave potential equal to

$$E_{1/2} = E^0 - 0.368 \frac{RT}{F} + \frac{2.303RT}{3F} \log ck_2 t \qquad (2)$$

where E^0 is the standard redox potential, c is the concentration of the redox active species, i_d is the diffusion-controlled limiting current, t is the drop time and k_2 is the rate constant of the radical dimerization. For this type of mechanism an increase of the concentration or the drop time by one order of magnitude leads to a shift of the half-wave potential by 19.7 mV to less negative values. Our experimental value of 21 ± 1 mV is very close to this predicted shift. The dependence of the electrode potential on the log $i^{2/3}\ i_d^{1/3}/(i_d - i)$ is shown in Fig. 1c and was constructed from the DC polarogram of 4.9 × 10^{-4} M DPBr in 0.1 M $TBAPF_6$ and DMSO. The dependence is indeed linear with the slope equal to 58 ± 2 mV, which is in good

agreement with the theoretically predicted value of 59.1 mV per decade for $n = 1$ (see Eq. (*1*)).

Further studies were performed using cyclic voltammetry (CV) at different scan rates from 0.01 to 32.8 V s^{-1} and at different concentrations. Figure 2a shows typical CV curves for reduction of 9.6×10^{-4} M DPBr in 0.3 M $TBAPF_6$ and DMSO at three different scan rates. These data confirm one single reduction process, which is chemically irreversible as reflected by the absence of a coupled oxidation process (anodic peak) upon scan reversal around –1.2 V. Instead, the oxidation wave of the product (most likely the dimer since the current reaches one half of the reduction current of the reactant) is observed around –0.35 V.

Additional proof for a bimolecular reaction following the reversible one-electron reduction comes from the logarithmic analysis of the semiintegrated voltammograms shown in Fig. 2b. The currents i were converted to the semiintegrated current I using the following transformation.

$$I = \frac{1}{\pi^{1/2}} \int_0^t \frac{i(v)}{(t - v)^{1/2}} \mathrm{d}v \qquad (3)$$

It has been shown[35,36] that a Nernstian charge transfer followed by a fast and irreversible dimerization leads to the expression

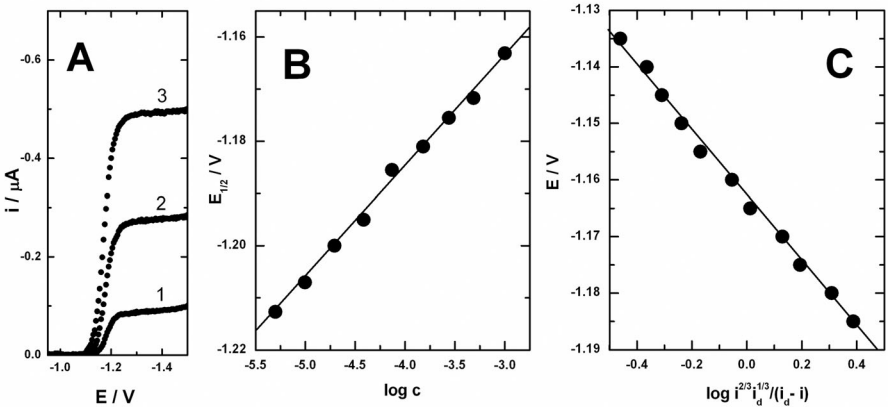

FIG. 1

Panel A: Sampled DC polarogram of 7.4×10^{-5} (1), 2.8×10^{-4} (2) and 4.9×10^{-4} M (3) DPBr in 0.1 M $TBAPF_6$ and DMSO. SMDE drop time was 2 s and electrode area 0.01036 cm^2. Panel B: Dependence of the half-wave potential $E_{1/2}$ on the logarithm of the DPBr concentration. Panel C: Logarithmic analysis of the DC polarogram of 4.9×10^{-4} M DPBr in 0.1 M $TBAPF_6$ and DMSO

$$E = E^0 + \frac{2.303RT}{3nF} \log \frac{2}{3} \frac{k_2}{FAD_0^{1/2}} + \frac{2.303RT}{nF} \log \frac{I_L - I}{i^{2/3}} \quad (4)$$

where E^0 is the standard redox potential, A is the electrode area, D_0 is the diffusion coefficient of the reactant, i is the measured current, I_L is the limiting semiintegrated current and other parameters have their usual meaning. Therefore, for the EC^2 type of mechanism the logarithmic analysis leads to a straight line with the same slope independent of both scan rate and the concentration. Figure 2b shows such a logarithmic analysis for curve *1* of Fig. 2a, which gives the slope 55 ± 2 mV. The dependence is linear and the slope is close to the theoretical value of 59.1 mV per decade. Finally, Fig. 2c shows how the parameter $i_p/v^{1/2}$ changes with the scan rate v. In the case of non-complicated reversible ET this parameter should stay constant, whereas Wopschall and Shain[37] showed that $i_p/v^{1/2}$ decreases with increasing $v^{1/2}$ if the product is weakly adsorbed on the electrode surface.

Exhaustive bulk electrolysis confirmed the consumption of one electron per DPBr molecule. Figure 3 shows the DC polarogram of the 4.16×10^{-3} M DPBr solution in 0.1 M $TBAPF_6$ and DMSO before and after exhaustive electrolysis at applied potential –1.40 V. Large area mercury pool was used as the working electrode. The color of the solution changed from light yellow to pale blue and after reoxidation at –0.25 V back to the original color. Ex-

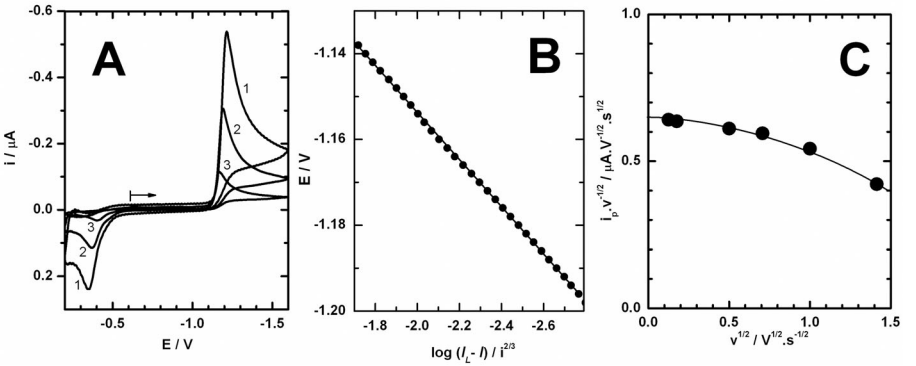

FIG. 2

Panel A: Cyclic voltammogram of 9.6×10^{-4} M DPBr in 0.3 M $TBAPF_6$ and DMSO at scan rate of 1 (1), 0.25 (2) and 0.03 V s^{-1} (3), respectively. Potential was scanned from –0.6 to –1.6 V and back to –0.2 V, followed by return to –0.6 V. HMDE of the area 0.00273 cm^2 was used. Panel B: Logarithmic analysis of the semiintegrated reduction currents of curve 1 in panel A. Panel C: Graph of the dependence $i_p/v^{1/2}$ vs $v^{1/2}$ constructed from cyclic voltammograms at different scan rates (see panel A), where i_p is the cathodic peak current and v is the scan rate

haustive electrolysis leads to the oxidation wave of the product around –0.45 V with height of the wave equal to approximately one half of the original wave of the reactant. The product after complete oxidation at –0.25 V

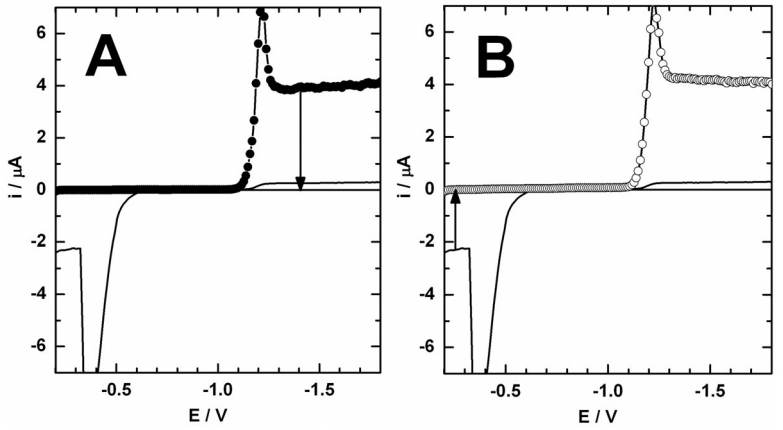

FIG. 3

Panel A: Sampled DC polarogram of 4.16×10^{-3} M DPBr in 0.1 M $TBAPF_6$ and DMSO before (●) and after (full line) exhaustive electrolysis at –1.40 V. Panel B: Sampled DC polarogram of the 4.16×10^{-3} M DPBr in 0.1 M $TBAPF_6$ and DMSO after (full line) exhaustive electrolysis at –1.40 V followed by reoxidation of previously reduced sample at –0.25 V (○). SMDE drop time was 2 s and electrode area 0.01036 cm^2

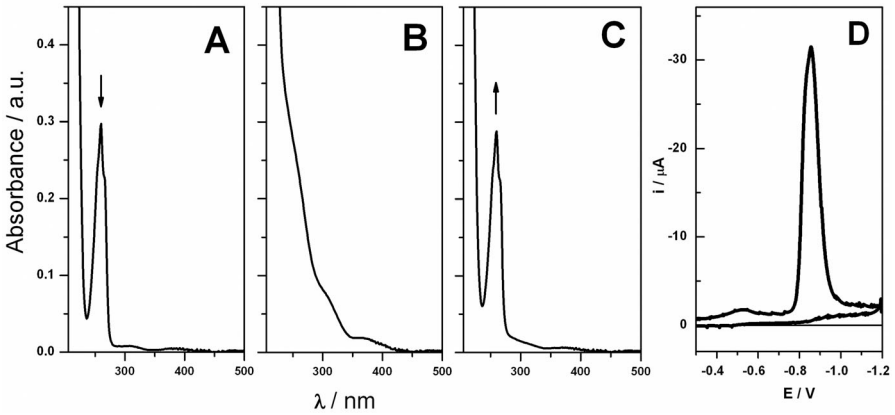

FIG. 4

UV-Vis absorption spectrum of 2.87×10^{-3} M DPBr in 0.2 M $TBAPF_6$ and dichloroethane obtained in the OTTLE cell after the double potential step from –0.4 (A) to –1.1 V (B) and back to +0.3 V (C). Time delay between individual steps was 100 s. The corresponding cyclic voltammogram in the OTTLE cell was obtained at scan rate 0.002 V s^{-1} (D)

gives the DC polarogram identical to the polarogram of the reactant. Charge consumed during reoxidation of the electrolytic product was equal to the charge consumed during reduction of DPBr at –1.40 V.

An independent experiment in the spectroelectrochemical cell (Fig. 4) using platinum mesh electrode and dichloroethane solvent confirmed that the reduction product is reoxidized back to the compound with the UV-Vis spectrum identical to the spectrum of the original DPBr reactant. UV-Vis spectra were measured up to 1000 nm wavelength, but no additional absorption peaks were observed in this range. Therefore, in the proposed reaction mechanism, the original DPBr reactant can be regenerated back by the oxidation of the reaction product (Scheme 2). Corresponding cyclic voltammogram in the OTTLE cell is shown in Fig. 4d.

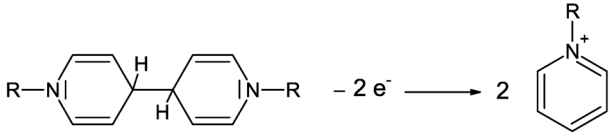

SCHEME 2

Further studies were focused on possible evidence of the DPBr adsorption (or its reduction product) on the electrode|electrolyte interface. Representative AC voltammograms are shown in Fig. 5 for the reduction of 9.6×10^{-4} M DPBr in 0.3 M $TBAPF_6$ and DMSO using two types of electrodes: static mercury drop electrode SMDE (Fig. 5a) or hanging mercury drop electrode HMDE (Fig. 5b) and measuring frequency 8 Hz at AC amplitude 5 mV. Curves labeled *Y′* and *Y″* represent the in-phase and out-of-phase admittance components, respectively. These measurements should reveal any possible adsorption effects. Even though the out-of-phase admittance components are in both cases smaller than the in-phase ones the graphs show marked dependence on the history of the experiment. In the case of SMDE, the mercury electrode is renewed before each potential increment (drop time 3 s), whereas this is not the case for HMDE electrode, keeping the time between individual potential increments equal to 3 s for both electrodes. Admittance data are different in both cases and indicate the presence of a weak adsorption process. A long term development of the *Y″* value with time (shown in Fig. 5 as the capacitance $C = Y''/2\pi f$) clearly shows the decrease in the differential capacitance of the solution|HMDE interface and points to the adsorption of the reduction product at the electrode surface. Analysis of the AC voltammetric data using the relationship between cotg ϕ and $\omega^{1/2}$, where ϕ is the faradaic phase angle and ω is the an-

gular frequency, confirms the EC type of mechanism, in which the electron transfer is reversible (data not shown)[38].

Finally, utilizing all the available experimental evidence the CV data were numerically simulated using a fully implicit finite difference method implemented within the DigiSim software and the best fit of the curve *1* of Fig. 2a is shown in Fig. 6 together with the mechanism employed. The following parameters produced the best fit of the experimental CV: E^{01} = –1.233 V, k_1 = 0.032 cm s^{-1}, E^{03} = –0.452 V, k_3 = 0.00028 cm s^{-1}, dimerization rate constant $k_2 = 5.3 \times 10^6$ l mol^{-1} s^{-1} and $K_{eq}^{dim} = 4.8 \times 10^{11}$ l mol^{-1} with diffusion coefficients of the monomer and dimer 4.5×10^6 and 3.5×10^6 cm^2 s^{-1}, respectively. We should stress that the objective of the fitting was to find a single set of parameter values that would provide the best average agreement between simulation and experiment for the entire range of the measured scan rates. These are the values reported above. If one compares, the best fits of the individual curves the standard redox potential value of the first electron transfer E^{01} can be obtained with relatively good precision and is in the range –1.233 ± 0.002 V, the same is true for k_1 and k_3 values, whereas k_2 provided best fits to individual curves in the range from 10^6 to 10^5 l mol^{-1} s^{-1} and K_{eq}^{dim} within the interval from 10^{10} to

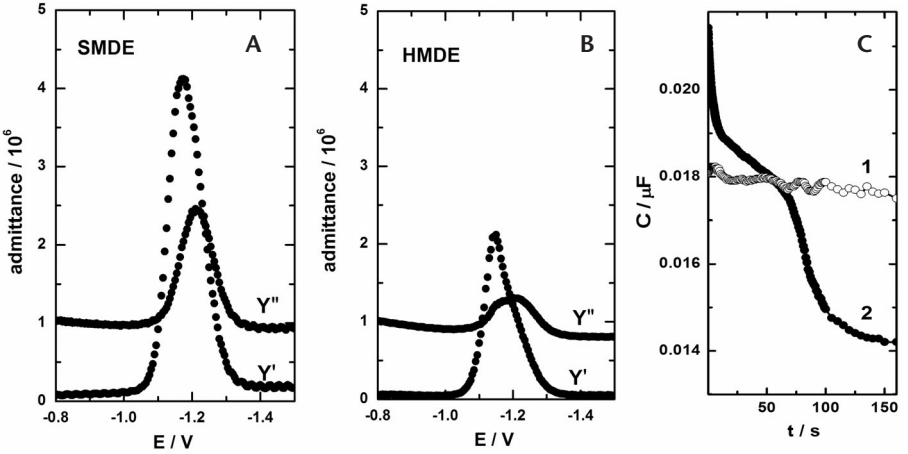

FIG. 5

AC voltammogram of 9.6×10^{-4} M DPBr in 0.3 M $TBAPF_6$ and DMSO using SMDE (A) or HMDE (B) obtained at frequency 8 Hz and AC amplitude 5 mV, drop time 3 s and electrode area 0.00273 cm^2. Curves labeled Y′ and Y″ represent the in-phase and out-of-phase admittance components, respectively. The differential capacitance of the solution|HMDE interface as a function of time was obtained at potential –1.0 (C, 1) and –1.35 V (C, 2) at frequency 160 Hz and amplitude 5 mV

10^{12} l mol^{-1}. Uncertainties reflect also the fact that the experimental curves include the presence of weak adsorption processes that are not accounted for by the simulation software. Value of the dimerization rate constant k_2 can be obtained independently from the DC polarographic data (see Eq. (*2*)) if one knows the standard potential of the electron transfer step. From the experimental dependence of the half-wave potential on the log c (see data in Fig. 1b) and assuming that $E^0 = -1.233 \pm 0.002$ V, one obtains k_2 in the range $(9 \pm 2) \times 10^6$ l mol^{-1} s^{-1}. This value is in reasonably good agreement with the dimerization rate constant obtained from the fitting of the cyclic voltammograms.

Electrochemical studies were complemented by the ex situ scanning tunnelling microscopy images of DPBr molecules adsorbed on the highly oriented pyrolytic graphite (HOPG) electrode surface. The deposition was done in the STM electrochemical cell at the open circuit potential, where the exposed HOPG area was limited to the area defined by the O-ring. After deposition time of several hours the excess DPBr was washed by copious amounts of pure acetonitrile solvent. The ex situ STM images were obtained using the air dried samples.

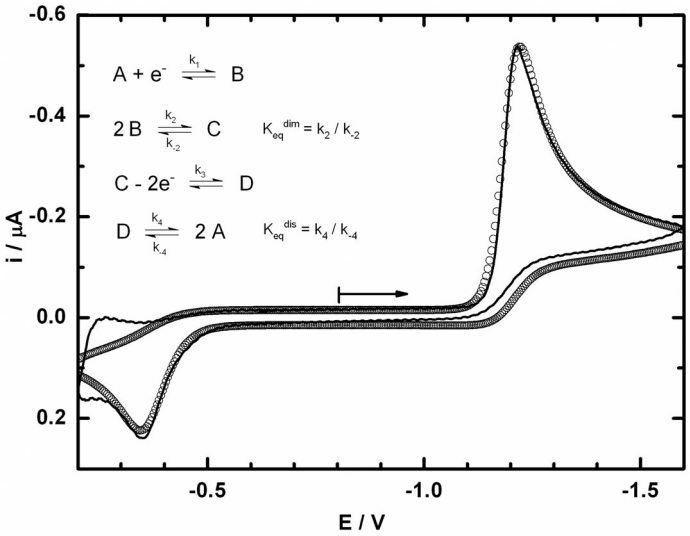

FIG. 6

Experimental (full line) and simulated (○) cyclic voltammograms of 9.6×10^{-4} M DPBr in 0.3 M $TBAPF_6$ and DMSO. Potential was scanned from –0.8 to –1.6 V and back to –0.2 V, followed by return to –0.8 V at scan rate 1 V s^{-1}. HMDE of the area 0.00273 cm^2 was used. Inset shows the reduction mechanism used for fitting

Figure 7 shows representative height images of the DPBr molecules on the electrode surface. As the deposition was not completed on the entire HOPG surface it was possible to find areas, where the HOPG substrate was imaged as well. These areas are seen in the bottom of the images 7a and 7c. More disordered character and higher mobility of DPBr molecules at the boundaries between adsorbate-covered and clean HOPG surface are clearly visible in both images as streaky and noisy areas lacking repeatable structure. Figure 7b also indicates that DPBr does not have only one type of arrangement on the HOPG surface in the absence of the electrode potential control. Several arrangements of molecules in the compact film are possible and may be linked to pyridinium moiety laying either flat on the electrode surface or laying in more upright orientation allowing maximum interaction between the pyridinium moieties on one hand and alkyl chains on the other. Size of the DPBr molecule was obtained as geometry optimized structure using computational software Spartan'08 (Wavefunction, Inc., USA). Length of the molecule is 1.84 nm and width (including associated bromide

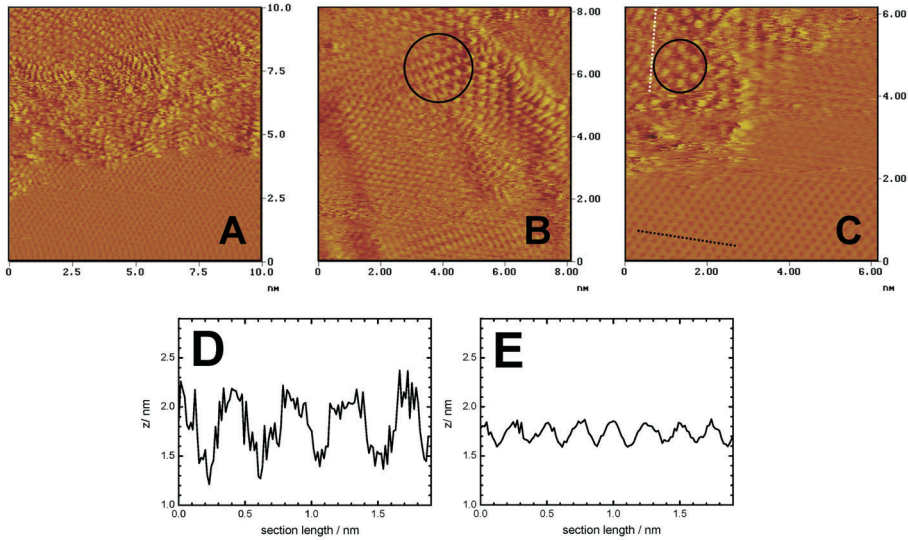

FIG. 7
The ex situ STM height images of the DPBr adsorption on HOPG electrode at three different locations: A (image size 10 × 10 nm^2, height scale 3 nm), B (image size 8 × 8 nm^2, height scale 3.5 nm) and C (image size 6 × 6 nm^2, height scale 4 nm), respectively. Experimental conditions: set point current 0.6 nA, bias voltage +20 mV, scan in the air using mechanically cut Pt-Ir 80/20 tip. Height profiles along the white dotted line (D) and black dotted line (E) in the image C

anion) is 0.43 nm. The average distance between the highest point of the bright spots of the adsorbed DPBr molecules in Fig. 7c and the bright spots corresponding to the HOPG surface carbon atoms is around 0.4 nm (see height profiles in Figs 7d and 7e) and cannot account for fully extended upright orientation of the DPBr molecules. One pattern indicated by circles in the images 7b and 7c repeats frequently. It is the hexagonal arrangement of bright spots on the top of the larger circular objects. Even though we know that STM images do not reflect directly the topography but rather indicate the local density of states (LDOS) it can be nevertheless speculated (based on the electrostatic concerns and assuming the size of individual DPBr molecules) that these features represent closely packed DPBr molecules with bromide anions visualized as bright spots in the height images.

CONCLUSIONS

We have shown that the reduction of 1-dodecylpyridin-1-ium bromide in dimethylsulfoxide solvent proceeds through reversible ET followed by a rapid dimerization of the radical intermediate. The dimerization rate constant $k_2 = 5.3 \times 10^6$ l mol^{-1} s^{-1} was obtained from the numerical simulation of the cyclic voltammograms and is in close agreement with the value obtained from the experimental DC polarograms. The in situ spectroelectrochemistry confirmed the dissociation of the dimer upon reduction yielding back the original reactant. Furthermore, AC admittance techniques demonstrated that the reduction mechanism is also complicated by weak adsorption of the dimer on the electrode|electrolyte interface. The ex situ STM imaging technique was used for visualization of DPBr molecules on the HOPG electrode surface.

This work was supported by the Grant Agency of the Academy of Sciences of the Czech Republic (IAA400400802), Czech Science Foundation (GACR 203/08/1157 and GACR 203/09/0705) and Ministry of Education, Youth and Sports of the Czech Republic (MEB041006).

REFERENCES

1. Haiss W., van Zalinge H., Higgins S. J., Bethell D., Höbenreich H., Schiffrin D. J., Nichols R. J.: *J. Am. Chem. Soc.* **2003**, *125*, 15294.
2. Li Z., Han B., Meszaros G., Pobelov I., Wandlowski T., Blaszczyk A., Mayor M.: *Faraday Discuss.* **2006**, *131*, 121.
3. Lee N. S., Shin H. K., Qian D. J., Kwon Y. S.: *Thin Solid Films* **2007**, *515*, 5163.
4. Pobelov I., Li Z., Wandlowski T.: *J. Am. Chem. Soc.* **2008**, *130*, 16045.

5. Leary E., Higgins S. J., van Zalinge H., Haiss W., Nichols R. J., Nygaard S., Jeppesen J. O., Ulstrup J.: *J. Am. Chem. Soc.* **2008**, *130*, 12204.
6. Bagrets A., Arnold A., Evers F.: *J. Am. Chem. Soc.* **2008**, *130*, 9013.
7. Wang Ch., Batsanov A. S., Bryce M. R., Martín S., Nichols R. J., Higgins S. J., García-Suárez V. M., Lambert C. J.: *J. Am. Chem. Soc.* **2009**, *131*, 15647.
8. Pospíšil L., Hromadová M., Fanelli N., Valášek M., Kolivoška V., Gál M.: *Phys. Chem. Chem. Phys.* **2011**, *13*, 4365.
9. Kolivoška V., Gál M., Pospíšil L., Valášek M., Hromadová M.: *Phys. Chem. Chem. Phys.* **2011**, *13*, 11422.
10. Lund H. in: *Organic Electrochemistry* (H. Lund and O. Hammerich, Eds), 4th ed., Chap. 18. Marcel Dekker, New York 1991.
11. Gaudiello J. G., Larkin D., Rawn J. D., Sosnowski J. J., Bancroft E. E., Blount H. N.: *J. Electroanal. Chem.* **1982**, *131*, 203.
12. Bonicelli M. G., Cardinali M. E., Carelli I.: *J. Electroanal. Chem.* **1982**, *131*, 345.
13. Mairanovskii S. G.: *Dokl. Akad. Nauk SSSR* **1956**, *110*, 593.
14. Kůta J., Pospíšil L., Smoler I., Girina G. P.: *J. Electroanal. Chem.* **1975**, *65*, 661.
15. Raghavan R., Iwamoto R. T.: *J. Electroanal. Chem.* **1978**, *92*, 101.
16. Volke J., Naarová M.: *Collect. Czech. Chem. Commun.* **1972**, *37*, 3361.
17. Carelli I., Cardinali M. E., Micheletti Moracci F.: *J. Electroanal. Chem.* **1980**, *107*, 391.
18. Naarová M., Volke J.: *Collect. Czech. Chem. Commun.* **1973**, *38*, 2670.
19. Khomchenko T. N., Nekrasov L. N.: *Elektrokhimiya* **1987**, *23*, 1134.
20. Toomey J. E.: *Electrochemical Dimerizations of Pyridinium Salts*, 1991, Eur No. EP0226319, http://www.freepatentsonline.com/EP0226319B1.html.
21. Kinoshita H., Uehara M., Nakaya J.: *Bulletin of University of Osaka Prefecture – Series A: Engineering and Natural Sciences* **1981**, *29*, 157.
22. Volke J., Dunsch L., Volkeová V., Petr A., Urban J.: *Electrochim. Acta* **1997**, *42*, 1771.
23. Mairanovskii S. G.: *Elektrokhimiya* **1967**, *3*, 1434.
24. Meunier-Prest R., Laviron E.: *J. Electroanal. Chem.* **1997**, *437*, 61.
25. Santhanam K. S. V., Elving P. J.: *J. Am. Chem. Soc.* **1973**, *95*, 5482.
26. Raghavan R., Iwamoto R. T.: *J. Electroanal. Chem.* **1978**, *92*, 101.
27. Yasukouchi K., Taniguchi I., Yamaguchi H., Shiraishi M.: *J. Electroanal. Chem.* **1979**, *105*, 403.
28. Volke J., Urban J., Volkeová V.: *Electrochim. Acta* **1994**, *39*, 2049.
29. Fujio K., Ikeda S.: *Langmuir* **1991**, *7*, 2899.
30. Wan-Badhi W. A., Palepu R., Bloor D. M., Hall D. G., Wyn-Jones E.: *J. Phys. Chem.* **1991**, *95*, 6642.
31. Krejčík M., Daněk M., Hartl F.: *J. Electroanal. Chem.* **1991**, *317*, 179.
32. http://www.reading.ac.uk/web/FILES/chemistry/F_Hartl_OTTLE_cells.pdf (downloaded 27th July 2011).
33. Hanuš V.: *Chem. Zvesti* **1954**, *8*, 702.
34. Heyrovský J., Kůta J.: *Základy polarografie*, pp. 272–273. Nakladatelství Československé akademie věd, Praha 1962.
35. Imbeaux J. C., Savéant J. M.: *J. Electroanal. Chem.* **1973**, *44*, 169.
36. Savéant J. M., Tessier D.: *J. Electroanal. Chem.* **1975**, *61*, 251.
37. Wopschall R. H., Shain I.: *Anal. Chem.* **1967**, *39*, 1514.
38. Hromadová M., Kolivoška V., Pospíšil L. in: *30th Modern Electrochemical Methods* (T. Navrátil and J. Barek, Eds), pp. 77–79. Best Servis, Prague 2010.